Does Atmospheric Cooling Drive the Gulf Stream Recirculation?*

RUI XIN HUANG

Department of Physical Oceanography, Woods Hole Oceanographic Institution, Woods Hole, Massachusetts

(Manuscript received 4 October 1989, in final form 24 November 1989)

ABSTRACT

A two-layer model for the recirculation is studied. Initially, a narrow jet of the upper layer moves eastward with the lower layer remaining stagnant. At $t = 0$ cold air flows over the narrow front region, all the moving water in the upper layer sinks to the lower layer with the momentum vertically well mixed within the lower layer. Thus, cooling creates an unbalanced eastward jet in the second layer and an unbalanced pressure field at a vertical density front. After the geostrophic adjustment, a high pressure center south of the front and a low pressure center north of the front are established. These pressure centers drive a much stronger barotropic eastward current slightly north of the pressure center and slow westward return flow in the far field both south and north of the front. Thus, cooling over a narrow stream can intensify an eastward jet and create recirculation gyres both north and south of the stream.

1. Introduction

In both the North Atlantic and North Pacific there are very strong recirculation gyres just south of the separated western boundary currents (Gulf Stream and Kuroshio). In the North Atlantic, there is the well-known "Worthington Gyre" (Worthington 1976). There is also a strong recirculation gyre north of the Gulf Stream (Hogg and Stommel 1986; Hogg et al. 1986). The maximum eastward mass fluxes in these eastward currents are several times larger than the maximum flux calculated based on linear Sverdrup dynamics. In the North Atlantic the mass flux increases rapidly downstream of Cape Hatteras and eventually reaches about 150 Sv. Theories based upon wind forcing only, either quasi-geostrophic or layered models, have been proposed for explaining the formation and dynamical structure of the recirculation. Many models can be traced back to the potential vorticity homogenization theory by Rhines and Young (1982). Although a large amount of low potential vorticity water exists in the oceans, the formation processes of these water masses is not yet clear. Comparing the streamline map by Worthington with the air–sea heat flux map by Bunker (1976), there seems a very tight link between recirculation and atmospheric cooling of the Gulf Stream. Eddy diffusion certainly plays some role; however, the dynamical role of thermal forcing is not well understood.

In this study we take a different approach, i.e., we emphasize the dynamical role of cooling in setting up the potential vorticity field. As shown in the numerical experiments by Cox and Bryan (1984) and Huang and Bryan (1987), cooling is responsible for destroying the high potential vorticity in the western boundary outflow region and creating a low potential vorticity water mass, while eddy diffusion further homogenizes the potential vorticity in the interior. This idea has been extended into a simple model of the subtropical gyre circulation in which cooling resets the potential vorticity of the western boundary outflow and allows a complete gyre without explicitly using friction (Cushman-Roisin 1987). Luyten and Stommel (1986) also considered a model with thermal forcing. However, both of these two models ignore the inertial terms in the horizontal momentum equations, so the vertically integrated mass flux is always subject to the Sverdrup constraint. As a result, these models predict that with cooling/heating there is no change in the barotropic mass flux. Therefore, a model with inertial terms and thermal forcing is needed to study the recirculation.

In fact, Worthington (1976) proposed a theory of the recirculation in his famous motto "Cold Wind—Two Gyres". He speculated that atmospheric cooling can set up an oceanic high pressure center and thus drive a recirculation. A close examination, however, shows that cooling cannot create a high pressure center without other dynamical processes. If an initially homogeneous and stagnant ocean is subject to a sudden local cooling, there will be no horizontal pressure gradient at the bottom, while the pressure will be low at the top due to the free surface difference. Obviously,

* Contribution No. 7271 from the Woods Hole Oceanographic Institution.

Corresponding author address: Dr. Rui Xin Huang, Department of Physical Oceanography, Woods Hole Oceanographic Institution, Woods Hole, MA 02543.

the high pressure center proposed by Worthington must be a result of horizontal mass redistribution during the geostrophic adjustment process after cooling.

Rossby (1938) studied the first example of geostrophic adjustment in which the pressure field was adjusted following an initially imposed narrow jet of velocity. Rossby's idea has been extended in many studies. According to the theory of geostrophic adjustment, for small scale perturbations (in terms of the Rossby deformation radius) the velocity field will basically remain and the pressure field will adjust towards an ultimate state geostrophically balanced with the velocity field; however, for large scale perturbations the initial pressure field will basically remain while the velocity field will adjust towards an ultimate state geostrophically balanced with the pressure field. Take, for example, Rossby's classic case. Assume that in a homogeneous ocean of depth H, a uniformly eastward velocity u_0 is suddenly imposed within a jet of width $2a$. According to Mihaljan's (1963) exact solution, the total eastward momentum remaining in the jet is $u_0H(1 - e^{-2a/\lambda})$, where $\lambda = \sqrt{gH}/f$ is the deformation radius. Thus, the ratio of remaining momentum to the initially imposed one is

$$R_m = \frac{\lambda}{2a}(1 - e^{-2a/\lambda}).$$

For $a \leqslant \lambda$,

$$R_m \approx 1 - \frac{a}{\lambda} + \frac{2a^2}{3\lambda^2}.$$

For $a \gg \lambda$, $R_m \to 0$. The scale dependence of geostrophic adjustment can be explained as follows. Since there was no horizontal pressure gradient to balance the eastward momentum, water particles move southward and create a high pressure center; however, in the process water particles also gain westward momentum due to Coriolis force. If the initial velocity perturbation has a small length scale, very little water movement is required for building up the final pressure field, thus the eastward momentum will basically remain unchanged. However, if the scale of the initial velocity perturbation is much larger than the deformation radius, much water has to be moved southward for building the pressure field to balance the velocity field, so most eastward momentum will be lost in the process of adjustment.

Stommel and Veronis (1980) studied several cases of geostrophic adjustment in which the velocity field is adjusted toward the initial pressure field set up by sudden cooling. As a natural step forward, we will study a model with both initial velocity and pressure perturbation in order to examine how the barotropic current and the high pressure center is established through cooling events. The model is formulated in section 2 and the result will be presented in section 3. Finally, we draw conclusions in section 4.

2. Model formulation

Our model is on an f-plane and has a flat bottom and two homogeneous layers of density ρ_1 and $\rho_2 = \rho_1 + \Delta\rho$. Initially, the second layer is stagnant and the upper layer moves eastward, see Fig. 1a. The x-axis of the local coordinates is in the downstream direction. To make a simple model, we assume that the upper layer thickness satisfies

$$\begin{aligned} H_1 &= 0, \quad \text{for} \quad 0 \leqslant Y < \infty, \\ H_1 &= H_{1\infty}(-Y/L_c)^{1/2}, \quad \text{for} \quad -L_c \leqslant Y < 0, \\ H_1 &= H_{1\infty}, \quad \text{for} \quad -\infty \leqslant Y < -L_c, \end{aligned} \tag{1}$$

where $H_{1\infty}$ is the undisturbed upper layer thickness at infinity, and the total depth of the model ocean is $H = (k + 1)H_{1\infty}$. We have chosen this profile so that the zonal momentum integrated within the upper layer is constant; thus, the zonal velocity in the second layer before the geostrophic adjustment will be uniform within a narrow jet. As we will see, this special profile makes the model analytically tractable.

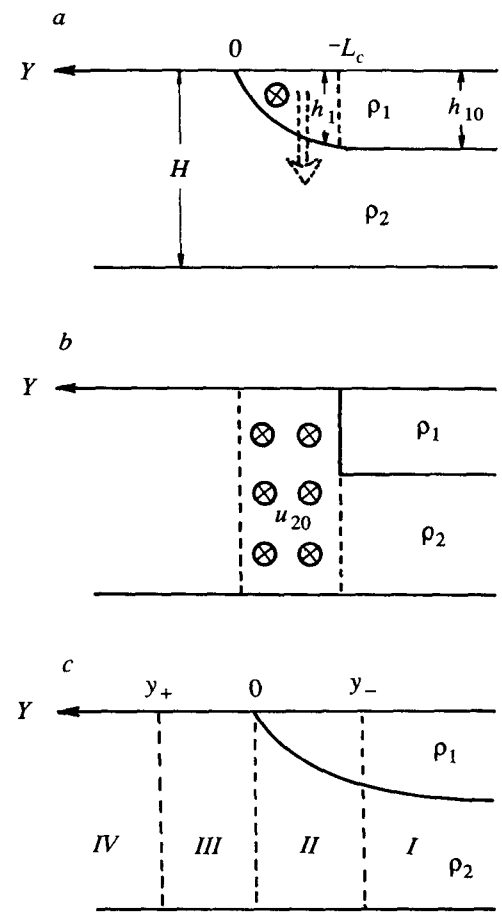

FIG. 1. Schematic structure of a two-layer model of the recirculation. (a) Before cooling; (b) after cooling and convective adjustment; (c) different regions for the final state solution after the geostrophic adjustment.

Suppose cold air suddenly flows over the ocean and cools all upper layer water north of $Y = -L_c$ to density ρ_2. After the cooling a fast convective mixing process, indicated by a dashed arrow in Fig. 1a, takes place and horizontal momentum is vertically well mixed within each water column. Now there is a vertical front between the upper layer and the lower layer, and a jet of eastward momentum in the second layer, Fig. 1b. Both the front and the velocity jet are geostrophically unbalanced, thus a geostrophic adjustment process will take place. This situation is a combination of the classical case of Rossby (1938) and the case discussed by Stommel and Veronis (1980). During the geostrophic adjustment the upper layer will spread northward, the lower layer will move southward and subduct underneath the upper layer. We choose the new outcropping position as the origin of a new coordinate. In the new coordinate the southern (northern) edge of the velocity jet in the second layer is y_- (y_+). Our analysis will follow the approach by Mihaljan (1963). Assuming the flow field is independent of x, the x-momentum equations are

$$\frac{du_1}{dt} = fv_1, \quad \frac{du_2}{dt} = fv_2. \tag{2}$$

Upon integrating from $t = 0$ to ∞, these lead to

$$u_1 = f(y - Y_1) + U_1(Y_1),$$
$$u_2 = f(y - Y_2) + U_2(Y_2), \tag{3}$$

where Y_1 and Y_2 are the initial positions of the water particles, U_1 and U_2 are the initial velocities. In the final state the downstream velocities are geostrophic

$$fu_1 = -g(h_{1y} + h_{2y}), \quad fu_2 = -g(\gamma h_{1y} + h_{2y}). \tag{4}$$

where f is the Coriolis parameter, g is the gravity, and $\gamma = \rho_1/\rho_2$. Mass conservation in each layer gives

$$h_1 = H_1 \frac{dY_1}{dy}, \quad h_2 = H_2 \frac{dY_2}{dy}, \tag{5}$$

where H_1 and H_2 are the initial layer thicknesses.

To facilitate the analysis we introduce the nondimensional variables

$$h_1 = H_{1\infty}h_1', \quad h_2 = kH_{1\infty}h_2', \tag{6}$$

$$y = \frac{\sqrt{gH_{1\infty}}}{f}y', \quad U_1 = \sqrt{gH_{1\infty}}u_{10}',$$
$$U_2 = \sqrt{gH_{1\infty}}u_{20}'. \tag{7}$$

Using these nondimensional variables and dropping primes, we derive two second-order ordinary differential equations

$$\frac{d^2Y_1}{dy^2} + k\frac{d^2Y_2}{dy^2} - Y_1 = -y - U_1, \tag{8}$$

$$\gamma\frac{d^2Y_2}{dy^2} + k\frac{d^2Y_2}{dy^2} - Y_2 = -y - U_2. \tag{9}$$

Note that in the general case k, U_1 and U_2 are functions of Y_1 and Y_2, so that these equations are nonlinear and difficult to handle analytically. We have constructed the model in such a way that k, U_1 and U_2 are constant in each region. In fact, there are four regions in the final state solution, Fig. 1c.

In Region I ($y \leqslant y_-$), both layers are in motion, $H_1 = H_{1\infty}$, $H_2 = kH_{1\infty}$, $U_1 = U_2 = 0$, so the general solutions which are finite at $y = -\infty$ can be written as

$$Y_1^{\mathrm{I}} = y + a_1e^{\alpha_+ y} + a_2e^{\alpha_- y}, \tag{10}$$

$$h_1^{\mathrm{I}} = 1 + a_1\alpha_+e^{\alpha_+ y} + a_2\alpha_-e^{\alpha_- y}, \tag{11}$$

$$Y_2^{\mathrm{I}} = y + b_1e^{\alpha_+ y} + b_2e^{\alpha_- y}, \tag{12}$$

$$h_2^{\mathrm{I}} = 1 + b_1\alpha_+e^{\alpha_+ y} + b_2\alpha_-e^{\alpha_- y}, \tag{13}$$

where

$$\alpha_\pm = \left[\frac{k + 1 \pm \sqrt{(k-1)^2 + 4k\gamma}}{2k(1-\gamma)}\right]^{1/2}. \tag{14}$$

In Region II ($y_- < y \leqslant 0$), both layers are in motion, $H_1 = H_{1\infty}$, $H_2 = (k + \gamma)H_{1\infty}$, $U_1 = 0$, $U_2 \neq 0$, so the general solutions can be written as

$$Y_1^{\mathrm{II}} = y + c_1e^{\beta_+ y} + c_2e^{-\beta_+ y} + c_3e^{\beta_- y} + c_4e^{-\beta_- y}, \tag{15}$$

$$h_1^{\mathrm{II}} = y + c_1\beta_+e^{\beta_+ y} - c_2\beta_+e^{-\beta_+ y} + c_3\beta_-e^{\beta_- y} - c_4\beta_-e^{-\beta_- y}, \tag{16}$$

$$Y_2^{\mathrm{II}} = y + d_1e^{\beta_+ y} + d_2e^{-\beta_+ y} + d_3e^{\beta_- y} + d_4e^{-\beta_- y} + U_2, \tag{17}$$

$$h_2^{\mathrm{II}} = 1 + d_1\beta_+e^{\beta_+ y} - d_2\beta_+e^{-\beta_+ y} + d_3\beta_-e^{\beta_- y} - d_4\beta_-e^{-\beta_- y}, \tag{18}$$

where

$$\beta_\pm = \left[\frac{k + \gamma + 1 \pm \sqrt{(k+\gamma-1)^2 + 4(k+\gamma)\gamma}}{2(k+\gamma)(1-\gamma)}\right]^{1/2}. \tag{19}$$

In Region III ($0 < y < y_+$), the upper layer vanishes, $H_2 = (k + \gamma)H_{1\infty}$, $U_2 \neq 0$, so the general solution is

$$Y_2^{\mathrm{III}} = y + e_1e^{\mu y} + e_2e^{-\mu y} + U_2, \tag{20}$$

$$h_2^{\mathrm{III}} = y + e_1\mu e^{\mu y} - e_2\mu e^{-\mu y}, \tag{21}$$

where

$$\mu = \left(\frac{1}{k+\gamma}\right)^{1/2}. \tag{22}$$

In Region IV ($y_+ < y < +\infty$), $H_2 = (k + \gamma)H_{1\infty}$, $U_2 = 0$, so the general solution is

$$Y_2^{\mathrm{IV}} = y + e_3e^{-\mu y}, \tag{23}$$

$$h_2^{\mathrm{IV}} = 1 - e_3\mu e^{-\mu y}. \tag{24}$$

Substituting these solutions into (8, 9), we find the relations between the coefficients

$$b_1 = \frac{\gamma\alpha_+^2}{1 - k\alpha_+^2} a_1, \quad b_2 = \frac{\gamma\alpha_-^2}{1 - k\alpha_-^2} a_2, \quad (25)$$

$$d_1 = \frac{\gamma\beta_+^2}{1 - (k+\gamma)\beta_+^2} c_1, \quad d_2 = \frac{\gamma\beta_+^2}{1 - (k+\gamma)\beta_+^2} c_2,$$

$$d_3 = \frac{\gamma\beta_-^2}{1 - (k+\gamma)\beta_-^2} c_3,$$

$$d_4 = \frac{\gamma\beta_-^2}{1 - (k+\gamma)\beta_-^2} c_4. \quad (26)$$

Since the upper layer outcrops at the origin of the local coordinates, we have

$$c_1\beta_+ - c_2\beta_+ + c_3\beta_- - c_4\beta_- = -1. \quad (27)$$

Matching conditions at y_-, 0, and y_+ are the continuity of Y_1, Y_2, h_1, and h_2, so that

$$a_1 e^{\alpha_+ y_-} + a_2 e^{\alpha_- y_-} = c_1 e^{\beta_+ y_-} + c_2 e^{-\beta_+ y_-} + c_3 e^{\beta_- y_-} + c_4 e^{-\beta_- y_-}, \quad (28)$$

$$b_1 e^{\alpha_+ y_-} + b_2 e^{\alpha_- y_-} = d_1 e^{\beta_+ y_-} + d_2 e^{-\beta_+ y_-} + d_3 e^{\beta_- y_-} + d_4 e^{-\beta_- y_-} + U_2, \quad (29)$$

$$a_1\alpha_+ e^{\alpha_+ y_-} + a_2\alpha_+ e^{\alpha_- y_-} = c_1\beta_+ e^{\beta_+ y_-} - c_2\beta_+ e^{-\beta_+ y_-} + c_3\beta_- e^{\beta_- y_-} - c_4\beta_- e^{-\beta_- y_-}, \quad (30)$$

$$k(1 + b_1\alpha_+ e^{\alpha_+ y_-} + b_2\alpha_+ e^{\alpha_- y_-}) = (k+\gamma)(1 + d_1\beta_+ e^{\beta_+ y_-} - d_2\beta_+ e^{-\beta_+ y_-} + d_3\beta_- e^{\beta_- y_-} - d_4\beta_- e^{-\beta_- y_-}), \quad (31)$$

$$d_1 + d_2 + d_3 + d_4 = e_1 + e_2, \quad (32)$$

$$d_1\beta_+ - d_2\beta_+ + d_3\beta_- - d_4\beta_- = e_1\mu - e_2\mu, \quad (33)$$

$$e_1 e^{\mu y_+} + e_2 e^{-\mu y_+} + U_2 = e_3 e^{-\mu y_+}, \quad (34)$$

$$e_1\mu e^{\mu y_+} - e_2\mu e^{-\mu y_+} = -e_3\mu e^{-\mu y_+}. \quad (35)$$

In addition, before the adjustment the width of the eastward velocity jet in the second layer is l_c (L_c, in dimensional form), i.e., $Y_2(y_+) - Y_2(y_-) = l_c$, so that

$$y_+ + e_1 e^{\mu y_+} + e_2 e^{-\mu y_+} = y_- + l_c + d_1 e^{\beta_+ y_-} + d_2 e^{-\beta_+ y_-} + d_3 e^{\beta_- y_-} + d_4 e^{-\beta_- y_-}, \quad (36)$$

Notice that the right edge of the second layer and the left edge of the upper layer were at the same location before adjustment, i.e., $Y_1(0) = Y_2(y_-)$, so that

$$c_1 + c_2 + c_3 + c_4 = y_- + b_1 e^{\alpha_+ y_-} + b_2 e^{\alpha_- y_-}. \quad (37)$$

The equation system (25)–(37) has 17 unknowns, it is linear in a_i, b_i, c_i, d_i, and e_i; however, it is transcendental in y_+ and y_-. Finding the solution of the state after geostrophic adjustment is reduced to solving two transcendental equations of two unknowns y_+ and y_-.

If the initial width L_c is less than the baroclinic deformation radius L_R, the eastward momentum jet of the second layer may be entirely "subducted" underneath the upper layer front, i.e. $y_+ < 0$. The solution for this case can be found by a similar approach through matching solutions over four regions. The problem involves solving a transcendental equation system of 23 unknowns. Since this case does not provide new physics, we will not discuss it in this paper.

3. Model results

To demonstrate the basic idea we have chosen the model's parameters to be typical of the Gulf Stream. The upper layer has an undisturbed thickness of $H_{1\infty}$ = 750 m, corresponding to the warm core of the Gulf Stream. Initially only the upper layer moves eastward within a narrow frontal zone of order of the baroclinic deformation radius

$$L_c \approx L_R = \frac{\sqrt{g\Delta\rho H_{1\infty}/\rho}}{f},$$

where $g\Delta\rho/\rho$ is 1.5 cm s^{-2}. We use an f-plane ocean model centered at 38.5°N. The total depth of the model ocean is 3 km. The model result of a case with $L_c = 1.1 L_R$ is shown in Fig. 2. A short dashed line in Fig. 2a depicts the initial position of the interface. When cooling takes place, all the moving water (left of the vertical dashed line) in the upper layer sinks to the second layer with momentum vertically well mixed. Right after convective adjustment the interface between the two layers becomes a vertical line: the vertical dashed line in Fig. 2a. Note that all the upper layer water left of this vertical line goes to the second layer. After the geostrophic adjustment the interface is depicted by a heavy solid line and the free surface is depicted by a thin solid line. Note that, to show the free surface elevation on the same map, we have defined an equivalent surface elevation by assuming that the entire water column is cooled to density of ρ_2 and the deviation from the mean sea surface has been exaggerated 1000 times. The most prominent feature is the high pressure center south of the front. The maximum free surface elevation is +0.10 m for the high pressure center.

The velocity distribution is depicted in Fig. 2b. There is a strong eastward velocity jet near the outcropping front in both layers. The eastward momentum in the upper layer is a result of Coriolis force since the upper layer moves northward in the process of geostrophic adjustment as can be seen in Fig. 2a. The eastward momentum in the second layer is the remaining part of the momentum dumped into the second layer during the cooling event. Since the second layer is subducted underneath the top layer, part of the eastward momentum is lost due to the southward motion in the

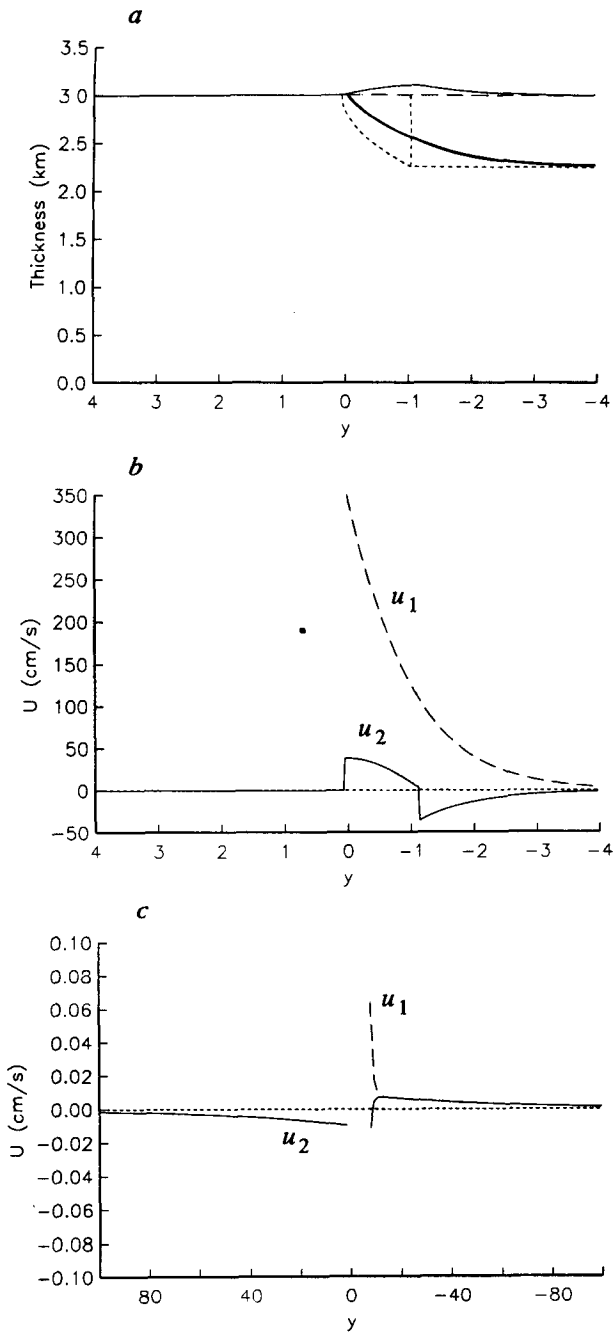

FIG. 2. A solution of the model. (a) Layer thicknesses distribution, y-coordinate in units of baroclinic deformation radius. The heavy solid line indicates the upper interface, the long dashed line indicating the mean upper surface, the thin solid line for the free surface, and the short dashed line depicts the upper interface before cooling with a vertical dashed line indicating the vertical front after cooling. Zonal velocity distribution of the model is shown in (b) and (c), a long dashed line indicates the upper layer velocity, a solid line depicts the lower layer velocity; (b) near field, (c) far field.

geostrophic adjustment process. A strong westward return flow develops in the second layer south of the front. In the far field, there is broad slow westward motion in the lower layer north of the front, but both layers move eastward far south of the front. Note that baroclinic structure exists only within several baroclinic deformation radii.

Therefore, the model shows that a barotropic high pressure center south of the front created during the geostrophic adjustment drives a tight recirculation south of the stream. The westward return flow is rather broad and much slower than the eastward jet. This westward velocity is superimposed on the wind-driven circulation of the interior ocean. Similarly, a much weaker (the minimum free surface elevation is only -0.0017 m, not visible in Fig. 2a) low barotropic pressure center north of the stream drives a recirculation north of the front; this northern recirculation may correspond to a tight recirculation north of the Gulf Stream (Hogg and Stommel 1986).

Integrated mass fluxes within each layer are the following: within the upper layer there is 42.3 Sv (Sv $\equiv 10^6$ m^3 s^{-1}) eastward. In the lower layer there is 0.6 Sv westward north of the low pressure center, another 27.7 Sv westward south of the high pressure center, and 32.5 Sv eastward between the two pressure extrema. The total eastward mass flux in both layers is 74.8 Sv. (We have not included the small contribution, about 0.5 Sv, from the eastward motion far south of the front where both layers move eastward.) Compared with the 46.8 Sv in the original one-moving layer solution, the ratio of the eastward momentum before and after the cooling, M_r is 1.60, i.e., the eastward momentum increases 60% due to the cooling.

As discussed in the introduction, the final state of the geostrophic adjustment depends on the length scale of the original disturbance. For large scale velocity perturbations alone, most of the original velocity field will disappear in the final state. In the present model the situation is a little more complicated. Initially, there was also an unbalanced northward free surface (pressure) jump at the southern edge of the unbalanced velocity jet. This initial pressure jump will contribute to the final pressure gradient required for geostrophy. In the present model, the initial velocity is inversely proportional to the initial length scale L_c, but the initial pressure remains the same. As a result, the total eastward momentum increases slightly to 79.5 Sv ($M_r = 1.70$) when L_c is five times as large as L_R, and for larger L_c the total eastward momentum declines.

As a comparison we have set up a second model in which an upper layer of constant depth covers the entire ocean and both layers are stagnant. At time $t = 0$, cold air comes and all the upper layer water north of $y = 0$ sinks to the second layer. In this case, initially there is perturbation only to the pressure, but not to the velocity. This case is similar to that of Stommel and Veronis (1980), with a minor difference that a free surface is included in our second model. The free surface elevation pattern is different from the previous case, Fig. 3a. Note that there is a low pressure center south of

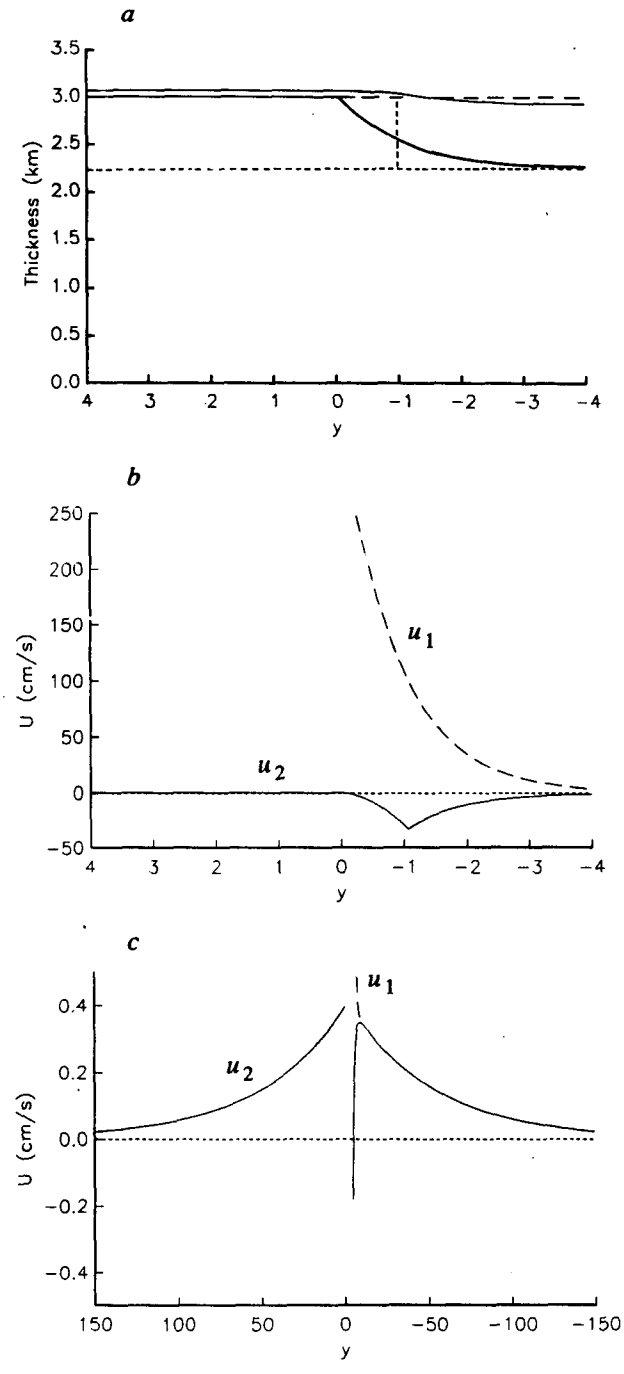

FIG. 3. A solution of the Stommel–Veronis model (including a free surface), see explanation of Fig. 2.

the front and a high pressure center to the north. The corresponding free surface elevation is −0.66 m for the low pressure center and +0.069 m for the high. The major difference from the model discussed above is in the velocity profile. Near the front the second layer moves westward, but north of the front it flows eastward. The integrated mass fluxes are: in the upper layer 43.7 Sv eastward; in the lower layer, 22.6 Sv eastward north of the outcropping front and another 36.2 Sv westward south of the front. Thus, the total eastward mass flux near the front is much smaller than in the previous case.

We have also studied a 2½-layer model in which only the top layer was initially in motion. Since the model formulation is very similar to the model above, it need not be included here. At time $t = 0$ cooling takes place and sends all moving water into the second layer. Geostrophic adjustment process takes place and the second layer begins to move. Assume that the reduced gravity across each interface is the same

$$\frac{\rho_3 - \rho_2}{\bar{\rho}} g = \frac{\rho_2 - \rho_1}{\bar{\rho}} g = 0.75 \text{ cm s}^{-2},$$

$$H_{1\infty} = 750 \text{ m}, \quad H = 3 \text{ km},$$

and the same initial width $1.1 L_R$. The solution is shown in Fig. 4. There is 25.2 Sv eastward flux in the upper layer and 17.2 Sv eastward flux in the second layer.

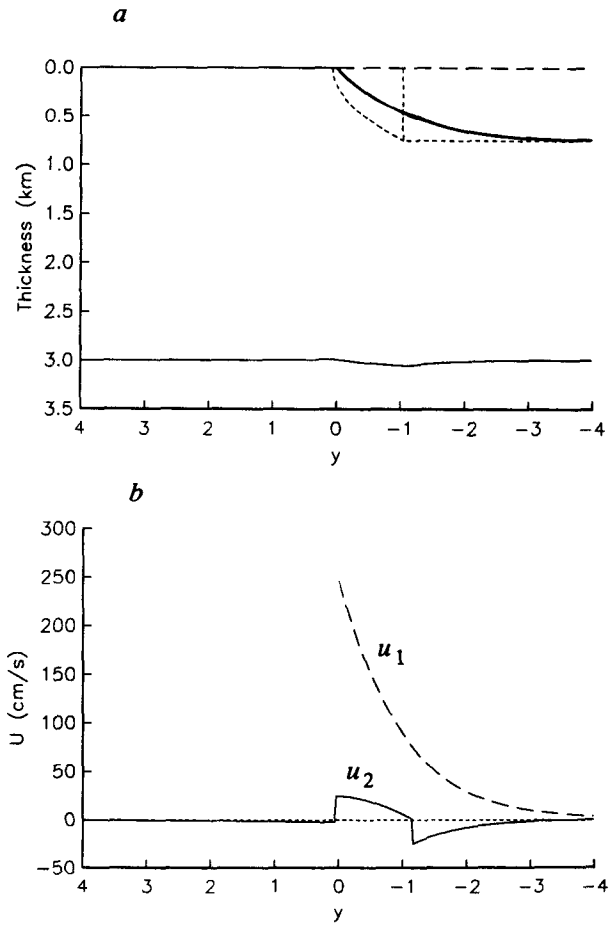

FIG. 4. Solution of a 2½-layer model. (a) Layer thickness distribution. (b) Velocity profile, a long dashed line indicates the upper layer velocity and a solid line depicts the second layer velocity.

Thus, the total eastward flux is 42.4 Sv. Compared with the 26.9 Sv for the initial state, the total eastward mass flux increases 58%. There is a broad return flow in the second layer north (and south) of the outcropping line which has flux of 3.9 Sv (12.3 Sv).

The major difference between models with a flat bottom and the model with a stagnant lowest layer is the scale separation. In models with a flat bottom, the barotropic deformation radius is about 30 times larger than the first baroclinic deformation radius. This scale separation gives rise to a mode of very large decay distance; thus, slow flows appear in both layers in the far field. Since the width of a front is much smaller than the barotropic deformation radius, the eastward momentum velocity initially imposed in the second layer tends to remain. For the model with a stagnant lowest layer, however, the scale separation is minor. As a result, the model behaves differently. First, the flow field is concentrated near the front within a few internal deformation radii. Second, the total eastward momentum decreases if the width of the stream before cooling, L_c, is larger than the deformation radius, and most of the eastward momentum transferred into the second layer is lost during the geostrophic adjustment. In fact, $M_r = 1.54$ for $L_c = 5.0$.

4. Conclusions

In the North Atlantic the recirculations are closely related to the 18°C water formation. Using a simple model we have demonstrated that by cooling a narrow stream the eastward momentum can be intensified. In the real ocean, cooling events take place one after the other. After each cooling episode, a huge amount of warm water in the upper layer sinks down to the layer below. Thus, cooling plays two major roles in the general circulation. First, horizontal momentum is transported downward during the convective adjustment. Second, at the middle depth, a low potential vorticity water mass is created during the process. After geostrophic adjustment, water moves southward and creates a high pressure center to the south and a low pressure center to the north. These two pressure centers drive strong recirculations both south and north of the stream. Although cooling takes place only during late winter, the high and low pressure centers built during the cooling season can remain for a long time before diffusion eliminates them. Since these barotropic pressure centers are associated with a vast amount of available potential energy, the decay time is very long. Before diffusion has consumed these pressure centers, the next cooling season comes and rebuilds them. Thus, the recirculations may stay there almost permanently with a small seasonal cycle in their strength.

The process of recirculation intensification in the oceans is highly idealized in our model; thus, the model results do not really match the situation in the North Atlantic. For example, the strength of the northern recirculation in the model is about $1 \sim 3$ Sv, much less than the observed value of 20 Sv. There is another apparent puzzle associated with the model. The process described here seems repetitive by nature; each cooling event can send some eastward momentum to the second layer and produce an additional eastward transport. Thus, after several cooling events the total eastward mass flux will be well over the observed volume of 150 Sv. There are many possible controlling factors which can limit the strength of the recirculation, such as the total heat loss to the atmosphere, the upstream/downstream variance of the structure, and the nonuniformity of the potential vorticity. For example, consider the case when the second layer is originally in motion, the adjustment process might behave quite differently. To unravel the puzzle above and overcome the shortcomings, the model needs some modifications.

First, we have studied the final state only, but not the geostrophic adjustment process itself. The speed of this process depends on the speed of the internal gravity waves. For a current 50 km wide, the geostrophic adjustment will reach a quasi-stationary state with a time scale of a day. Therefore, for time much longer than days and without getting into detail, the geostrophic adjustment process can be thought of as an instantaneous phenomenon.

Second, we have discussed a very special case in order to find a simple analytical solution. The initial velocity profile of the upper layer used in the present model has singularities at both ends. These singularities can be removed by using a general profile so that the layer-integrated momentum is a linear function of Y. This general case also leads to linear potential vorticity equations with analytical solutions. However, using a linear profile can only remove a singularity at one side. Therefore, we have chosen the simple case discussed above. It seems very interesting to study the general case where both layers were initially in motion and have nonuniform potential vorticity. Such a model can be studied numerically, yielding solution that shows the wave motions during the geostrophic adjustment.

Third, the present model assumes one-dimensional structure. In the North Atlantic, the strength of the recirculation increases gradually in the downstream direction. The three-dimensional structure of the recirculation must be taken into consideration in further study.

Finally, cooling and convective adjustment processes need to be studied in order to understand the dynamic role of atmospheric cooling. It is important to note that the present model emphasizes the importance of using numerical schemes that conserve momentum during the convective adjustment process. The implication for numerical modeling, especially for the case involved with cooling near a front, will be explored in further study.

Acknowledgments. Dr. Henry Stommel made important suggestions in the formulation of this problem. I have also learned about the structure of the recirculations through discussions with him. This work was supported by OCE88-08076 from National Science Foundation.

REFERENCES

Bunker, A. F., 1976: Computations of surface energy flux and annual air-sea interaction cycles of the North Atlantic Ocean. *Mon. Wea. Rev.*, **104,** 1122–1140.

Cox, M. D., and K. Bryan, 1984: A numerical model of the ventilated thermocline. *J. Phys. Oceanogr.*, **14,** 674–687.

Cushman-Roisin, B., 1987: On the role of heat flux in the Gulf Stream–Sargasso Sea subtropical gyre system. *J. Phys. Oceanogr.*, **17,** 2189–2202.

Hogg, N. G., R. S. Pickart, R. M. Hendry and W. J. Smethie, Jr., 1986: The northern recirculation gyre of the Gulf Stream. *Deep–Sea Res.*, **33,** 1139–1165.

——, and H. Stommel, 1986: On the relation between the deep circulation and the Gulf Stream. *Deep–Sea Res.*, **32,** 1181–1193.

Huang, R. X., and K. Bryan, 1987: A multilayer model of the thermohaline and wind-driven ocean circulation. *J. Phys. Oceanogr.*, **17,** 1909–1924.

Luyten, J. R., and H. Stommel, 1986: Gyres driven by combined wind and buoyancy flux. *J. Phys. Oceanogr.*, **16,** 1551–1560.

Mihaljan, J. M., 1963: An exact solution of the Rossby adjustment problem. *Tellus,* **15,** 150–154.

Rhines, P. B., and W. R. Young, 1982: A theory of the wind-driven circulation. I. Mid-ocean gyres. *J. Mar. Res.*, **40**(Suppl.), 559–596.

Rossby, C. G., 1938: On the mutual adjustment of pressure and velocity distributions in certain simple current systems, II. *J. Mar. Res.*, **1,** 239–263.

Stommel, H., and G. Veronis, 1980: Barotropic response to cooling. *J. Geophys. Res.*, **85,** 6661–6666.

Worthington, L. V., 1976: On the North Atlantic circulation. *The Johns Hopkins Oceanogr. Stud.*, No. 6, 110 pp.